Proc. Natl. Acad. Sci. USA
Vol. 93, pp. 7446–7451, July 1996
Chemistry

Photo-induced inactivation of viruses: Adsorption of methylene blue, thionine, and thiopyronine on Qβ bacteriophage

STEFFEN JOCKUSCH*, DENIS LEE†, NICHOLAS J. TURRO*, AND EDWARD F. LEONARD†

*Department of Chemistry, Columbia University, New York, NY 10027; and †Department of Chemical Engineering, Materials Science, and Mining Engineering, Columbia University, New York, NY 10027

Contributed by Nicholas J. Turro, April 5, 1996

ABSTRACT **The adsorption of cationic organic dyes (methylene blue, thionine, and thiopyronine) on Qβ bacteriophage was studied by UV-visible and fluorescence spectroscopy. The dyes have shown a strong affinity to the virus and some have been used as sensitizers for photo-induced inactivation of virus. In the methylene blue concentration range of 0.1–5 μM and at high ratios of dye to virus (greater than 1000 dye molecules per virion), the dyes bind as aggregates on the virus. Aggregation lowers the efficiency of photoinactivation because of self-quenching of the dye. At lower ratios of dye to virus (lower than 500 dye molecules per virion), the dye binds to the virus as a monomer. Fluorescence polarization and time-resolved studies of the fluorescence support the conclusions based on fluorescence quenching. Increasing the ionic strength (adding NaCl) dissociates bound dye aggregates on the virus and releases monomeric dye into the bulk solution.**

Two broad techniques have been used for eliminating viral contamination in blood products: removal and inactivation. The former has been partially achieved by washing, filtration, or adsorption (1). The latter has utilized heat, intrinsically active chemical agents, photo- and γ-irradiation without chemical addition, and photo-irradiation in the presence of sensitizing agents that are usually inactive until irradiated (2–6). For inactivation to preserve sensitive bystander molecules or cells, a very high degree of specificity for the virus must be obtained. In general, photo-irradiation in the presence of sensitizing agents is the only method that has yet approached the requisite specificity, in part because the sensitizer can be concentrated on the virus before it is activated. The sensitizing agent must have a high binding constant and bind specifically to a viral component: its lipid envelope (when present), its protein coat, or its genome. It must also have a path by which it can reach this component, as well as time to do so. Any coreactant (e.g., oxygen) must also have a path by which it can reach the reaction site. Inactivation may occur either because photo-induced damage renders the virus unable to enter a prospective host cell or because the virus is unable to replicate after entry because its genome has been rendered defective.

We have selected methylene blue (MB) and its derivatives thionine (Th) and thiopyronine (TP) as prototype sensitizing agents (Fig. 1) for virus inactivation. These dyes have high *in vitro* binding affinity to nucleic acids, a feature that appears to confer their microbiocidal and virucidal activity (7, 8). MB is known as an antivirucidal compound, and it is at least competitive with other agents in minimizing undesirable effects. Its chemical and biological properties have been thoroughly studied (7), the optical absorption is optimum for the blood banking application, and it is currently being used clinically for photoinactivation of fresh frozen plasma in Europe (9). Inferring from the high binding affinity of MB, Th, and TP to nucleic acids and from the quenching of the fluorescent dye singlet excited states by the nucleic acid bases (10–12), we examined whether a similar quenching mechanism occurred in the MB/virus system. Bacteriophage Qβ, an icosahedral single-stranded RNA phage, was selected for this preliminary study in spite of many differences between it and mammalian viruses because of its ability to grow to high titers, its ease of assay, and the extensive information available about its structure, replication mechanism, and cloning.

The availability of an easy assay for MB binding is important for understanding the viral photoinactivation process and the reasons for incomplete inactivation. In this study, the equilibrium binding of cationic organic dyes MB, Th, and TP to Qβ bacteriophage was examined using photochemical methods. The effects of salt concentration (ionic strength) on the phage/MB binding equilibrium were also examined.

EXPERIMENTAL METHODS

Dyes. MB (MB^+Cl^- = MB) (Aldrich) was recrystallized from ethanol/water, 4:1 (vol/vol). Th (Th^+Cl^- = Th) was isolated from a commercial product (Th^+OAc^-, Fluka) by salting out with NaCl three times and recrystallizing from water and ethanol. TP (TP^+Cl^- = TP) (Fluka) was twice recrystallized from ethanol. Hydrogen chloride associated with crystalline TP (TP^+Cl^- × ½ HCl) was removed by heating at 100°C *in vacuo* at 0.1 torr (1 torr = 133 Pa) (13).

Transformation of *Escherichia coli* NP20 and Generation of Qβ Phage. *E. coli* NP20 (tet^r) was transformed with plasmid p^+QβWT (gifts of D. Mills, SUNY Downstate Brooklyn) to generate wild-type cloned Qβ phage. In the transformation, 50 μl of competent *E. coli* NP20 was added to 1 μl of plasmid p^+QβWT (concentration of 1 mg/ml, suspended in 10 mM Tris·HCl, pH 7.5/1 mM EDTA) at 0°C. After 20 min, cells were heat shocked at 42°C for 1 min and immediately chilled to 0°C with subsequent addition of 0.9 ml of sterile broth. After 5 min, the mixture was incubated at 37°C for 10 min. For plating of the transformed cells, 0.95 ml of the mixture was added to 3.5 ml of top agar at 45°C [TYGS medium (14)], gently mixed, plated onto a Petri dish with bottom agar, and incubated overnight at 37°C.

The overnight solid culture showed confluent lysis and a wild-type cloned Qβ culture was prepared from plate lysates by adding 5 ml of sterile broth to the lysed surface of the plate. After 1 h, the liquid sterile broth was removed to a sterile tube and 50 μl of chloroform was added. The culture was centrifuged (200 × *g*, 20 min), the pellet was discarded, and the supernatant was titrated (final titer, 10^{11} plaque-forming units/ml).

Growth and Purification of Qβ Phage. Standard microbiological procedures for *E. coli* K91 and phage growth and phage purification were used. *E. coli* K91 host (gift of P. Model, Rockefeller University, New York) was grown for 2–3 h in TYG medium (14) in a shaking water bath at 37°C until reaching logarithmic-phase growth ($OD_{660} \approx 0.44$). Phage Qβ were allowed to infect this culture. After 2.5 h of shaking incubation at 37°C, the bacteria were lysed with chloroform (2 μl/ml)/lysozyme (100 μg/ml) (Sigma, L-7651)/50 mM EDTA. Cellular debris was removed by centrifugation (200 ×

Abbreviations: MB, methylene blue; Th, thionine; TP, thiopyronine.

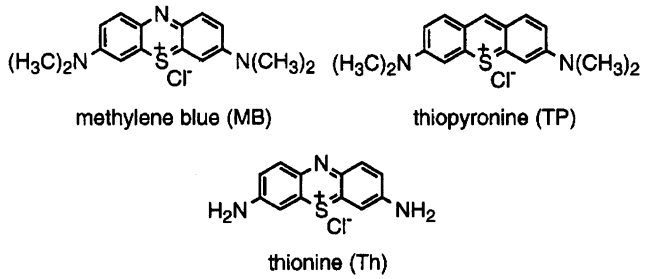

FIG. 1. Structures of MB, Th, and TP.

g) for 20 min. The supernatant was assayed and found always to contain 10^{11} plaque-forming units/ml.

Bacterial DNA in the centrifuged lysate was digested with DNase I, RNase-free (GIBCO/BRL), according to the manufacturer's instructions. The solution was filtered (0.22-μm pore size, Millipore), washed twice (20 mM Tris·HCl/100 mM NaCl, pH 5.3), and concentrated using a Centriprep-100 concentrator (M_r 100,000 cut-off, Amicon). The resulting virus titer was 10^{12} plaque-forming units/ml.

Viral particles were precipitated from solution with 3 M $(NH_4)_2SO_4$ and were collected by centrifugation at 3000 × *g* for 20 min. The precipitate was resuspended with a minimum volume of H_2O, filtered (0.22-μm pore size), further washed with H_2O, and concentrated using the Centriprep-100 concentrator. The concentrate was further purified in a CsCl gradient, by admixture with CsCl (ρ = 1.4 g/ml), and ultracentrifugation at 50,000 rpm in a Beckman ultracentrifuge L8-55 for 24 h at 25°C. The phage band was removed, double-washed, and concentrated in Centriprep-100 concentrators.

Quantification of Phage Particles. Purified concentrated Qβ particles were diluted 1:20, and their UV-absorption was measured at 260 nm (Beckman DU-64). The number of Qβ particles was calculated using published values of the extinction coefficient and molecular weight of Qβ: A_{260} = 8.01 $mg^{-1}\cdot ml^{-1}$ and a molecular weight of 4.2 × 10^6 (15).

Spectroscopic Measurements. MB, Th, and TP fluorescence intensities were measured in a Spex Fluorolog 1680 0.22-m double spectrometer, a Spex FluoroMax-2 spectrometer, or a Perkin–Elmer LS50B luminescence spectrometer. Optical absorption spectra were measured either on a Hewlett–Packard 8452A diode array spectrophotometer or a Perkin–Elmer Lambda 19 UV–visible–near infrared (UV/vis/NIR) spectrometer. The experiments were conducted by serial addition of known amounts of Qβ to a dye solution in a cuvette. For each addition, the dye/phage solution was incubated for at least 2 min before taking fluorescence and optical absorption measurements. The fluorescence polarization experiments were performed on the Spex FluoroMax-2 spectrometer using Glan Thompson polarizers.

A Continuum PY61–10 Nd-YAG laser system was used for excitation at 532 nm (≈0.5 mJ per 30-ps pulse) and a Hamamatsu streak scope C4334 system with Hamamatsu software was used for time-resolved fluorescence detection and data acquisition. This technique allows collection of fluorescence lifetimes and real-time kinetic quenching data in the fluorescence time regime relevant for the examination of the dyes (0.1–10 ns) (16).

MB Binding Curve Calculations. Fluorescence intensity data were used to compute a MB to Qβ binding curve. The calculations effectively defined the disappearance of fluorescence with a fraction of the MB originally in solution that had migrated to a nonfluorescent bound phase (MB_{bound}) associated with the added phage. The concentration of MB remaining free (MB_{free}) in the solution was thus taken to be directly proportional to the remaining fluorescence intensity. Binding curves were plotted as the ratio of MB_{bound}/phage versus the concentration of MB_{free} in solution using data from five experiments that differed in their initial MB concentrations.

RESULTS AND DISCUSSION

The MB monomers free in aqueous solution possess a strong optical absorption at 666 nm [ε = 82,000 $M^{-1}\cdot cm^{-1}$ (10)] and a weak fluorescence [Φ_f^{free} = 0.02 (10)] (Figs. 2 and 3, spectra a). When small amounts of Qβ were added to a MB solution, the optical absorption at 666 nm decreased (Fig. 2, spectra b and c) and simultaneously absorption around 610 nm increased. This absorption corresponds to that observed with MB aggregates (17–19) and can be clarified by subtraction of spectra a and e from spectrum c in Fig. 2, yielding spectrum f. In the presence of polyanions, MB has previously been shown to form large aggregates bound to the surface of the polyanion (18); these are readily detectable on the absorption spectra by a hypsochromic shift from the dye monomer and dimer. The aggregation or dimerization of MB in aqueous solutions in the absence of polyelectrolyte can occur only at relatively high dye concentrations (dimerization constant: 4.71 × 10^3 M^{-1}) (20). At the dye concentrations used in this study, MB did not show significant dimerization or aggregation in the absence of virus.

At high concentrations of Qβ (>5 × 10^{-9} M) the optical density at 666 nm reaches a minimum and starts to increase as additional Qβ are added to the system. This increase is caused by the monomeric adsorption of dye to the virus particles and is accompanied by the disappearance of aggregates. A concomitant bathochromic shift of about 14 nm is observed, indicating that the monomerically adsorbed MB is in an environment different from MB monomer in aqueous solution.

The change in optical absorption for an increase in Qβ concentration is accompanied by a decrease in MB fluorescence (Fig. 3 *Right*). This is caused by two different processes: (*i*) Fluorescence intensity decreases due to self-quenching of MB dimers and aggregates (21) [Fig. 3 *Right* shows that the amounts of monomeric and aggregated MB measured by UV–visible and fluorescence intensity follow essentially identical trends at low Qβ phage concentrations (<5 × 10^{-9} M).] (*ii*) The fluorescence of MB monomers intercalated into the viral RNA is quenched because of dye interactions (such as electron transfer) with nucleic acid bases. At high concentrations of Qβ phage (>5 × 10^{-8} M), the second process dominates. Previous reports (10, 11, 22) have shown that MB bound to poly(dG-dC) does not emit fluorescence while MB intercalated between the base pairs of poly(dA-dT) emits a

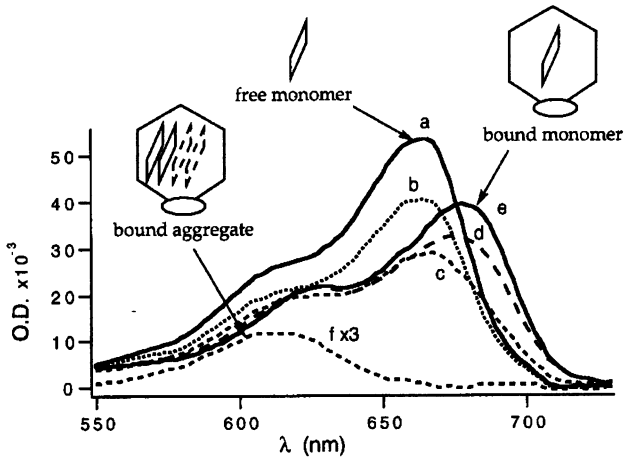

FIG. 2. Optical absorption of MB (7 × 10^{-7} M) in the presence of the following amounts of Qβ (× 10^{-9} M): 0 (spectrum a), 0.12 (spectrum b), 2.5 (spectrum c), 8.9 (spectrum d), and 18 (spectrum e). Spectrum f corresponds to the bound aggregates, calculated by subtraction of spectra a and e from spectrum c.

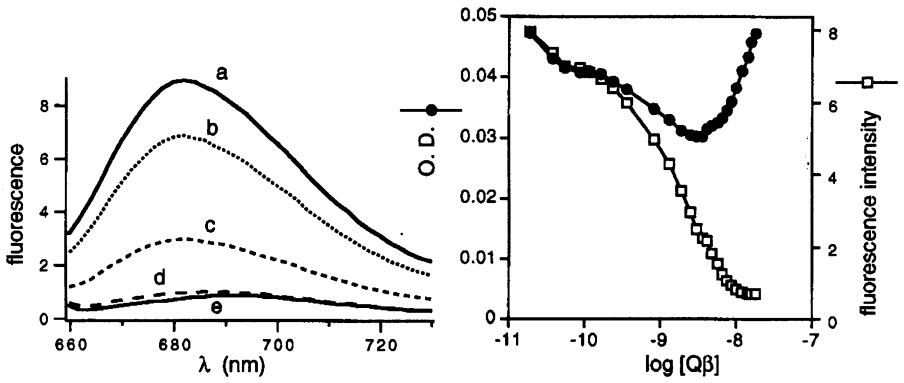

FIG. 3. Quenching of MB fluorescence by addition of Qβ phage ([MB] = 7×10^{-7} M, λ_{ex}=650 nm). (*Left*) Fluorescence spectra at different Qβ concentrations (see Fig. 2). (*Right*) Intensity of MB fluorescence (arbitrary units) at 682 nm (right axis) and optical density at the absorption maximum (left axis) versus Qβ phage concentration.

strong bathochromically shifted fluorescence (10, 11, 23). The difference in fluorescence intensities may be caused by the different oxidation potentials of the bases. In the case of poly(dG-dC), the reduction potential of the excited MB is high enough for electron transfer quenching and consequent oxidation of the guanosine residue (11). A corresponding reaction does not develop with poly(dA-dT). Two other possible mechanisms have been reported for the fluorescence quenching of MB by nucleic acid bases, hydrogen abstraction (10) and low-laying charge transfer state (24). It has been shown that MB preferentially intercalates next to G·C base pairs (10, 25) and that G·C base pairs quench MB fluorescence; therefore, RNA containing Qβ phage should quench most of MB fluorescence. MB monomer bound to Qβ phage possesses a fluorescence quantum yield of $\Phi_f^{bound} = 0.0013$ [$\Phi_f^{free} = 0.02$ (10)]. This fluorescence quantum yield indicates that not all MB is bound next to G·C base pairs. However, the fluorescence is attributed to bound MB and not to low amounts of MB remaining free in the bulk solution for the following reasons: (*i*) The fluorescence is shifted bathochromicaly (about 10 nm) compared with that of the free dye. (*ii*) The fluorescence excitation spectrum, the precursor of the fluorescence emission, also shows this bathochromic shift (about 10 nm). (*iii*) The fluorescence polarization value *P* (26) obtained from excitation with linear polarized light is significantly higher for the bound than for the free dye ($P^{free} = 0.11$; $P^{bound} = 0.39$). This high polarization value shows a restricted freedom of movement, most likely caused by binding of MB monomers to the virus.

Fig. 4 shows that the amount of MB apparently abstracted from solution by each added Qβ is initially very large, perhaps as much as 10^4 MB molecules per Qβ. These high levels of aggregation appear to be determined primarily by virus concentration and to occur at low values of virus concentration. They appear not to be determined primarily by the concentration of free MB (since in the different experiments the large MB/Qβ ratios occur at widely different MB concentrations). At higher virus concentrations the MB/Qβ ratios fall and the data conform to a concentration-sensitive Langmuir-like isotherm.

In accord with these observations, it is postulated that aggregation occurs on the outside of the virus particle and represents a balance between an aggregation process driven by the free MB concentration and a disaggregation process, second order in virus concentration, resulting from collisions of virus particles carrying aggregates with each other. When these collision rates are high, aggregation is unimportant and the principal cause of abstraction of MB from solution is its monomeric binding to sites on the virus, quite possibly to viral nucleic acid. This adsorption appears to involve an estimated 800 sites per Qβ.

A quantitative model incorporating these observations and assumptions was developed. The model requires (*i*) that equilibrium coverage of primary sites occurs rapidly, (*ii*) that aggregates form on each MB-covered site at a rate proportional to the free MB concentration and the difference between a maximum and the actual number of MB molecules per aggregate that are already occupied, and (*iii*) that each collision between viruses removes a fraction x of the aggregated MB on the viruses. Thus the aggregation of MB to Qβ can be described as:

$$r_a = k_a\left(\frac{C_{MB}}{K + C_{MB}}\right)C_{MB}(n - q)\sigma,$$

while the disaggregation is described as

$$r_d = k_d x C_v \theta,$$

where r_a is the adsorption rate of MB per virus, r_d is the desorption rate of MB per virus, k_a is the association constant, k_d is the dissociation constant, K is a Langmuir parameter, C_{MB} is the concentration of free MB in solution, C_v is the concentration of Qβ in solution, σ is the number of MB sites per Qβ particle, n is the number of MB molecules involved in one aggregate, θ is the fraction of sites occupied by MB, and x is the fraction of MB removed per collision. In equilibrium, $r_a = r_d$, yielding for θ,

$$\theta = \frac{n}{1 + \left[\frac{k_d(K + C_{MB})x}{k_a(C_{MB})^2\sigma}\right]C_v}.$$

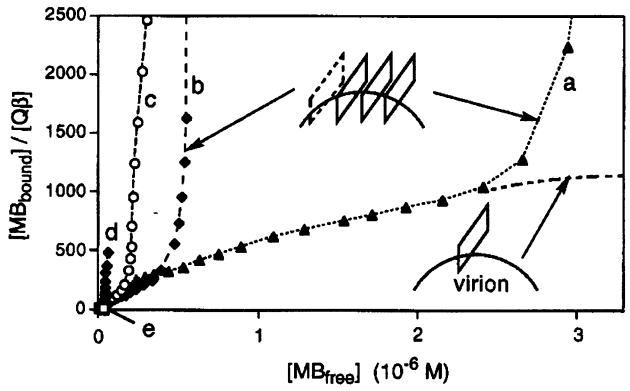

FIG. 4. Binding plot of the MB/Qβ system for the following initial concentrations of MB (μM) = 3.5 (a), 0.7 (b), 0.35 (c), 0.07 (d), and 0.035 (e). The ratio of the bound MB (monomers or aggregates) to Qβ versus the concentration of free MB is shown.

Table 1. Singlet energies (E^s), reduction potentials of the ground state (E^0_{red}), and first excited singlet state (E^s_{red}), fluorescence live times of the free dyes (τ_f^{free}), and fluorescence quantum yields of the free monomers (Φ_f^{free}) and bound monomers (Φ_f^{bound}) of the dyes used in this work

Parameter	MB	Th	TP
E^2, eV	1.84*	2.03*	2.21†
E^0_{red}, V	−0.05‡	−0.11‡	−0.17‡
E^s_{red}, V§	1.79	1.92	2.04
τ_f^{free}, ps	380*	320*	1700¶
Φ_f^{free}	0.02‖	0.047**	0.2††
Φ_f^{bound}	0.0013¶	0.0018¶	0.057¶
$\Phi_f^{bound}/\Phi_f^{free}$	0.07	0.04	0.29
P^{free}	0.11¶	0.09¶	0.04¶
P^{bound}	0.39¶	0.36¶	0.26¶

*Ref. 11.
†Ref. 27.
‡Ref. 27, measured vs. NHE and E_o(SCE) = 0.27.
‡NHE, normal hydrogen electrode; SCE, saturated calomel electrode.
§$E^s_{red} = E^s + E^0_{red}$.
¶Measured in this work.
‖Ref. 10.
**Ref. 28.
††Ref. 29.

The term $(K+C_{MB})/C_{MB}$ replicates the saturation behavior of the monomerically bound dyes. The collision factor, x, scales the aggregate breakdown consequent to the addition of increasing amounts of Qβ to the system. The appearance of C_v in these equations, which are formulated per virus, represents the second-order interactions between Qβ phage.

Thionine and Thiopyronine. The dyes Th and TP have structures similar to MB (Fig. 1) but show higher singlet energies and lower reduction potentials (Table 1). These differences may account for slight differences in binding properties of dye to virus. Optical absorption and fluorescence experiments with Th and TP were performed as with MB. All showed equivalent adsorption and aggregation behavior to Qβ (Fig. 5). At lower concentrations of Qβ, all three dyes showed a strong tendency to aggregate on the virus.

At high Qβ concentrations (>5 × 10^{-9} M) and dye concentrations between 0.5 and 5 μM (dye/phage ratios < 500), all three dyes were bound as monomers. All three dyes showed similar saturation of monomeric sites in the Langmuir-like isotherm portion of Fig. 4. Th has been reported to intercalate better than MB with nucleic acids [poly(dG·dC)]$_2$: K^{MB} = 1.0 × 10^6 M^{-1}, K^{Th} = 1.6 × 10^6 M^{-1} (11)], but our results show no difference in dye monomer binding to virus. For all three dyes, the optical absorption was bathochromically shifted from that of the free dye in solution. Th and TP also did not fluoresce in their aggregated phases because of self-quenching (21). The decrease in fluorescence intensity at low concentrations of Qβ followed the concentration of free dissolved dye (Figs. 3 and 5). A fluorescence of bound monomeric dye is observed for all three dyes, but the yield of this fluorescence (Φ_f^{bound}) differs among them (Table 1). The ratio between Φ_f^{bound} and Φ_f^{free} reflects the reactivity of the bound dye in its singlet excited state. This ratio increases in the order of Th < MB < TP (Table 1), implying a decrease in the reactivity of the singlet excited states of the bound dye monomers in this order. The higher reactivity of excited Th^{bound} singlets over MB^{bound} states can be explained by the higher singlet energy (E^s) of Th, which causes Th to have a higher excited state reduction potential (E^s_{red}) (Table 1). Previous reports (10, 11) have shown that MB quenching by electron transfer occurs only when it is intercalated close to guanine nucleotides but not when its neighbors are adenine nucleotides. It also has been reported (11) that Th is quenched by adenine nucleotides, consistent with its higher singlet energy. This explanation is also consistent with the lower ratio of Φ_f^{bound} to Φ_f^{free} for Th in comparison with MB. It is unclear why TP possesses the highest quantum yield ratio (Table 1). Its high singlet energy (E^s) causes a high reduction potential in the excited state (E^s_{red}). Thus TP in its singlet excited state should be easily quenched by most nucleotide bases. But it is reported that TP intercalated into calf thymus DNA also possesses a hypsochromically shifted strong fluorescence (30).

For each of the dyes studied, the bound monomers possess a significantly higher fluorescence polarization value than that of the free dye (Table 1). This higher polarization value implies restricted freedom of movement in the bound state. As expected, both polarization values for TP (P^{free} and P^{bound}) are lower than the corresponding values for MB and Th because of the longer fluorescence lifetime of the free and the bound TP.

In addition to the steady-state experiments, time-resolved fluorescence spectra were recorded for TP by excitation at λ_{ex} = 532 nm with 30-ps pulses. Fig. 6 shows fluorescence decays and spectra at different phage concentrations. The steady-state and time-resolved spectra both present similar bathochromically shifted emission from monomer dye bound to Qβ (Fig. 6). The fluorescence intensities of different time-resolved spectra are not comparable to each other because of the experimental method. Fig. 7 also shows the optical absorption spectrum at each Qβ concentration used for the time-resolved study. The free TP monomer in aqueous solutions (a) possesses a fluorescence lifetime, τ_f^{free}, of 1.7 ns. When a small amount of virus is added, the optical absorption of the free dye monomer decreases and the hypsochromically shifted absorption of bound dye aggregates can be observed (b of Fig. 6 *Upper Right*). The time-resolved fluorescence spectrum (spec-

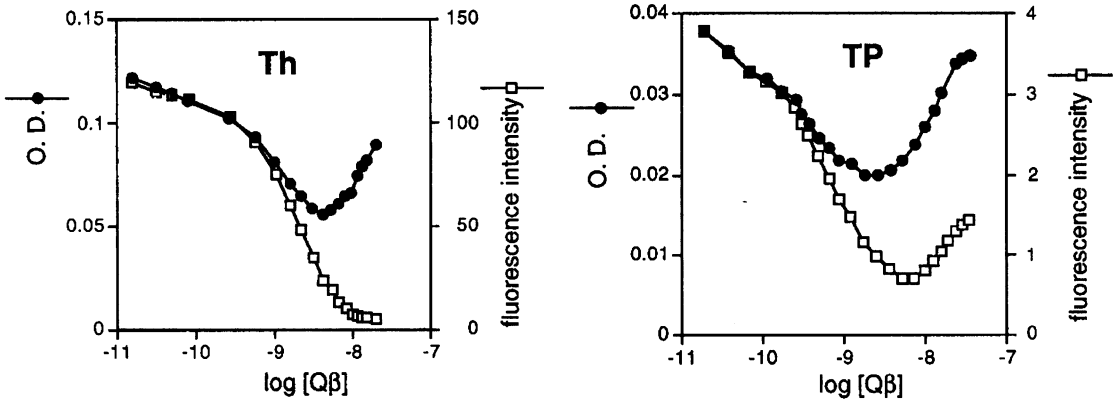

FIG. 5. Quenching of Th (*Left*) and TP (*Right*) fluorescence by addition of Qβ phage ([Th] = 2 × 10^{-6} M, λ_{ex}=598 nm; [TP] = 1 × 10^{-6} M, λ_{ex}=532 nm). Intensity of Th and TP at fluorescence maximum (arbitrary units) (right axis) and at maximum optical density (left axis) versus Qβ concentration is shown.

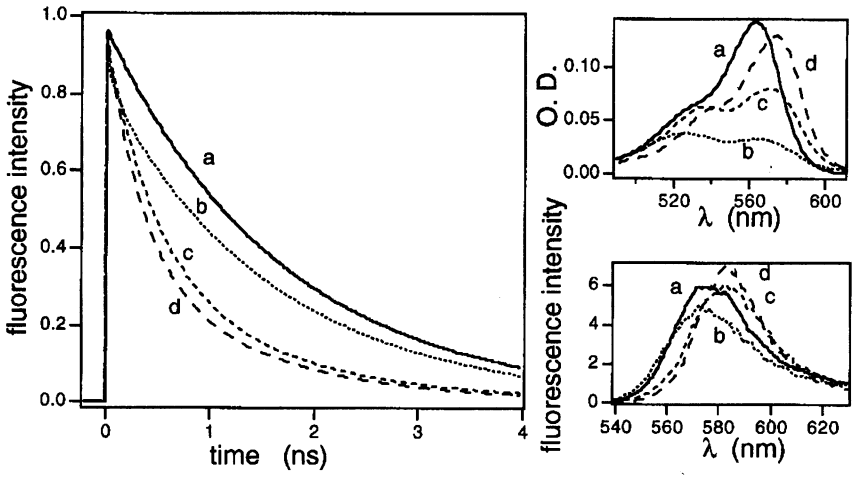

FIG. 6. Irradiation of aqueous solutions containing TP (1×10^{-5} M) and different amounts of Qβ [[Qβ] ($\times 10^{-9}$ M) = 0 (spectrum a), 5 (spectrum b), 30 (spectrum c), and 130 (spectrum d)] with a 30 ps flash (λ_{ex} = 532 nm). (*Left*) Fluorescence decay at 560 to 600 nm. (*Upper Right*) Optical absorption spectra. (*Lower Right*) Time-resolved fluorescence spectra at the end of the flash (integration time, 1 ns) is shown.

trum b) and the fluorescence decay (b) are very similar to those of the free TP monomer (a). At higher concentrations of Qβ, almost all of the dye molecules become distributed on the virus at the expense of the TP aggregates. The optical absorption and fluorescence of the bound monomer can be observed (spectrum d). The fluorescence time is significantly shorter (τ_f^{bound} = 0.4 ns) than that of the free dye. Spectra c in Fig. 6 lie between spectra b and d, which suggests that both aggregates and bound monomer are present. With fluorescence alone, only the bound and free monomers could be detected. While the fluorescence spectra and decay are strongly influenced by the bound monomer, a small amount of free monomer in the bulk solution is seen to cause a hypsochromic broadening of the fluorescence spectrum c and a small increase of the fluorescence lifetime compared with spectrum d.

Influence of Ionic Strength. Since blood plasma is about 0.15 M in electrolytes, the influence of ionic strength on the adsorption of MB to viruses is of interest. Ionic strength affects both aggregated and monomeric forms of binding.

To study the effect of ionic strength on MB aggregates, the optical absorption and fluorescence of an aqueous solution containing MB and Qβ were recorded at different concentrations of NaCl (Fig. 7). In the absence of NaCl, a large fraction of the MB appeared to exist as bound aggregates, and little monomer could be detected (Fig. 8, spectrum b). When the concentration of NaCl was increased, the fluorescence intensity and the optical absorption of the free MB increased (c–f). At [NaCl] = 0.1 M, almost no aggregates could be detected (spectrum f). The optical absorption and fluorescence intensity measurements and the fluorescence excitation spectra of the MB/Qβ/NaCl mixture ([NaCl] = 0.1 M) were similar to those of free monomer in water solution without Qβ. These results show that as the solution's ionic strength increased, dye molecules previously bound to viruses as aggregates were released as monomers to the aqueous bulk solution. This finding is consistent with previous reports (18) in which dye aggregates bound on polyelectrolytes were reported to be dissociated by KCl.

Ionic strength also influences monomeric binding. The mode of MB binding (intercalative or nonintercalative) on DNA or RNA depends on ionic strength (31–33). Qβ phage, which is composed of RNA, behaves like the polynucleotides at different ionic strengths (31–33). To study these effects with Qβ, the optical absorption and fluorescence of an aqueous solution containing MB and Qβ were recorded at different concentrations of NaCl (Fig. 8). In the absence of NaCl, almost all MB was bound to the virus as monomer (spectrum b). When the concentration of NaCl increased, the fluorescence of the free MB increased (spectra c and d) and the peak of the optical absorption shifted back to the position of the free monomer dye (spectrum a). In addition, the fluorescence excitation spectra of both the free monomer and the MB/Qβ/NaCl system ([NaCl] = 0.1 M) are almost identical. These results show that monomerically bound MB was released to the aqueous phase as a result of the increase in ionic strength.

CONCLUSION

The use of organic dyes as sensitizers for the inactivation of viruses in human blood products requires that the sensitizers show a high affinity to the virus. The cationic organic dye MB and its analogs Th and TP show such an affinity for bacteriophage Qβ, probably by association with viral nucleic acids, possibly with coat protein. At low Qβ concentrations ($<5 \times 10^{-9}$ M) and dye concentrations between 0.5 and 5 μM (dye/phage ratios > 1000), the dyes aggregate on the virus but this mode of association may be ineffective in viral inactivation because of self-quenching of the excited state of the dye. Both dye concentration and, surprisingly, the concentration of virus determine whether dye binds to the virus as monomer or aggregate.

Ionic strength strongly influences both monomeric adsorption and aggregation to virus. Increasing the ionic strength destroys virus-bound dye aggregates and releases bound dye

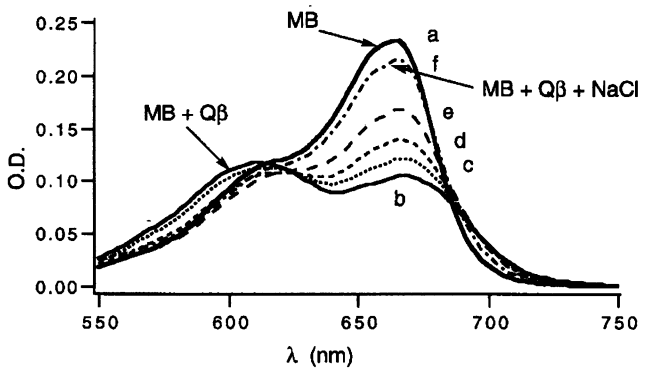

FIG. 7. Optical absorption of MB (3.5×10^{-6} M) in the absence (spectrum a) and presence of Qβ (8.8×10^{-9} M) (spectra b–f) and in the following amounts of NaCl ($\times 10^{-3}$ M): 0 (spectrum a), 0 (spectrum b), 0.1 (spectrum c), 1.8 (spectrum d), 10 (spectrum e), and 100 (spectrum f).

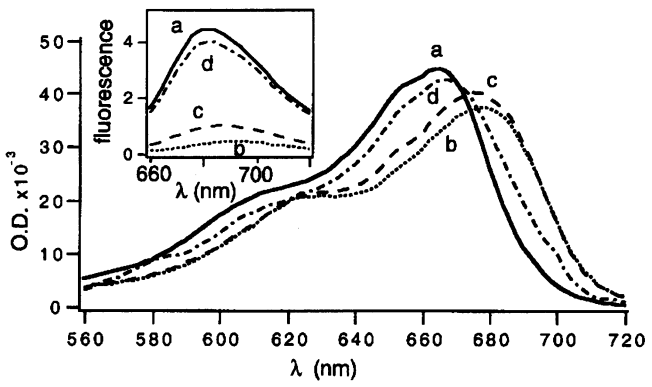

FIG. 8. Optical absorption and (*Inset*) fluorescence spectra of MB (7×10^{-7} M) in the absence (spectrum a) and presence of Qβ (6×10^{-7} M) (spectra b–d) and the follwoing amounts of NaCl: 2×10^{-4} M (spectrum c) and 8×10^{-2} M (spectrum d).

monomer into the bulk solution, a phenomenon of particular interest, since blood products generally have a high ionic strength.

We thank J.C. Scaiano (University of Ottawa, Canada) for the generous use of the time resolved fluorescence spectroscopy setup for these experiments and W. M. Nau and N. Mohtat for their help in performing the time resolved fluorescence experiments. We thank C. Hamish Young (Columbia University), D. Mills (State University of New York, Brooklyn), and P. Model (Rockefeller University) for their discussion and provision of phage procedures. D.L. and E.F.L. thank Baxter International and donors to the Artificial Organs Research Fund at Columbia University for their generous support. N.J.T. and S.J. thank the Air Force Office of Scientific Research and the National Science Foundation for their generous support of this research. S.J. also thanks the German Academic Exchange Service for a postdoctoral fellowship.

1. Wagner, S. J., Friedman, L. I. & Dodd, R. Y. (1991) *Transf. Med. Rev.* **5,** 18–32.
2. Gard, S. (1957) in *The Nature of Viruses*, eds. Wolstenhome, G. E. W. & Millar, E. C. P. (Little Brown, Boston), pp. 123–146.
3. Dodd, R. Y., Moroff, G., Wagner, S., Dabay, M. H., Dorfman, E., George, V., Ribeiro, A., Shumaker, J. & Benade, L. E. (1991) *Transfusion* **31,** 483–490.
4. Horowitz, B., Wiebe, M. E., Lippin, A. & Stryker, M. H. (1985) *Transfusion* **25,** 516–522.
5. Lin, L., Wiesehahn, G. P., Morei, P. A. & Corash, L. (1989) *Blood* **74,** 517–525.
6. Lin, L., Londe, H., Hanson, C. V., Wiesehahn, G., Isaacs, S., Cimino, G. & Corash, L. (1993) *Blood* **82,** 292–297.
7. Tuite, E. M. & Kelly, J. M. (1993) *J. Photochem. Photobiol. B* **21,** 103–124.
8. Mueller-Breitkreutz, K., Mohr, H., Briviba, K. & Sies, H. (1995) *J. Photochem. Photobiol. B* **30,** 63–70.
9. Mohr, H., Lambrecht, B. & Chmitt, H. (1993) in *Virological Safty Aspects of Plasma Derivatives*, ed. Brown, F. (Karger, Basel), Vol. 81, pp. 177–183.
10. Atherton, S. J. & Harriman, A. (1993) *J. Am. Chem. Soc.* **115,** 1816–1822.
11. Tuite, E., Kelly, J. M., Beddard, G. S. & Reid, G. S. (1994) *Chem. Phys. Lett.* **226,** 517–524.
12. Enescu, M. & Lindqvist, L. (1995) *Photochem. Photobiol.* **62,** 55–59.
13. Winter, G. & Steiner, U. (1980) *Ber. Bunsenges. Phys. Chem.* **84,** 1203–1214.
14. Atlas, R. M. & Parks, L. C. (1993) *Handbook of Microbiological Media* (CRC, Boca Raton, FL), p. 959.
15. Overby, L. R., Barlow, G. H. D., Jacob, M. & Spiegelman, S. (1966) *J. Bacteriol.* **91,** 442–448.
16. Nau, W. M., Cozens, F. L. & Scaiano, J. C. (1996) *J. Am. Chem. Soc.* **118,** 2275.
17. Jockusch, S., Turro, N. J. & Tomalia, D. A. (1995) *Macromolecules* **28,** 7416–7418.
18. Shirai, M., Nagatsuka, T. & Tanaka, M. (1977) *J. Polym. Sci. Polym. Chem. Ed.* **15,** 2083–2095.
19. Neumann, M. G. & Hioka, N. (1987) *J. Appl. Polym. Sci.* **34,** 2829–2836.
20. Ruprecht, J. & Baumgaertel, H. (1984) *Ber. Bunsenges. Phys. Chem.* **88,** 145–150.
21. Yuzhakov, V. I. (1979) *Russ. Chem. Rev. (Engl. Transl.)* **48,** 1076–1091.
22. Lober, G. J. (1981) *Luminescence* **22,** 221–265.
23. Dunn, D. A., Vivain, H. L. & Kochevar, I. E. (1991) *Photochem. Photobiol.* **53,** 47–56.
24. Enescu, M., Krim, L., Lindqvist, L. & Tieqiang, W. (1994) *J. Photochem. Photobiol. B* **22,** 165–169.
25. Tanaka, S., Baba, Y. & Kagemonto, A. (1981) *Macromol. Chem.* **182,** 1475–1480.
26. Barton, J. K. (1993) *Methods Enzymol.* **226,** 577–591.
27. Timpe, H.-J. & Neuenfeld, S. (1992) *J. Chem. Soc. Faraday Trans.* **88,** 2329–2336.
28. Archer, M. D., Ferreira, M. I. C., Porter, G. & Tredwell, C. J. (1977) *Nouv. J. Chim.* **1,** 9–12.
29. Morita, M. & Kato, S. (1969) *Bull. Chem. Soc. Jpn.* **42,** 25–35.
30. Lalitha, S. & Haug, A. (1972) *Biochemistry* **11,** 1590–1595.
31. Norden, B. & Tjerneld, F. (1982) *Biopolymers* **21,** 1713–1734.
32. Antony, T., Atreyi, M. & Rao, M. V. R. (1993) *J. Biomol. Struct. Dyn.* **11,** 67–81.
33. Hagmar, P., Pierrou, S., Nielson, P., Norden, B. & Kubista, M. (1992) *J. Biomol. Struct. Dyn.* **9,** 667–679.